ESSENTIAL ROLES OF THE *SPPRA* FRUCTOSE-PHOSPHATE PHOSPHOHYDROLASE OPERON IN CARBOHYDRATE METABOLISM AND VIRULENCE EXPRESSION BY *STREPTOCOCCUS MUTANS*

Lin Zeng and Robert A. Burne[#]

Department of Oral Biology, University of Florida, Gainesville, Florida, USA

Running title: Adaptation to sugar-phosphate stress

Key words: fructose metabolism, sugar-phosphate stress, xylitol, biofilm, sugar-phosphate phosphohydrolase

[#]Corresponding Author:

1395 Center Drive, Gainesville, Florida 32610

Phone: 352 273-8850

FAX: 352 273-8829

Email: rburne@dental.ufl.edu

Abstract

The dental caries pathogen *Streptococcus mutans* can ferment a variety of sugars to produce organic acids. Exposure of *S. mutans* to certain non-metabolizable carbohydrates (e.g., xylitol) impairs growth and can cause cell death. Recently, the presence of a sugar-phosphate stress in *S. mutans* was demonstrated using a mutant lacking 1-phosphofructokinase (FruK) when fructose was present in the environment. Here we studied an operon in *S. mutans, sppRA,* which was highly expressed in the *fruK* mutant. Biochemical characterization of a purified, recombinant SppA protein indicated that it possessed hexose-phosphate phosphohydrolase activity, with preferences for fructose-1-phosphate (F-1-P) and fructose-6-phosphate (F-6-P). SppA activity was stimulated by Mg^{2+} and Mn^{2+}, but inhibited by NaF. SppR, a DeoR-family regulator, repressed the expression of the *sppRA* operon in the absence of fructose-derived metabolites. Constitutive expression of *sppA,* via a plasmid, greatly alleviated fructose-induced stress in a *fruK* mutant, and enhanced resistance to xylitol. Furthermore, accumulation of F-1-P not only induced *sppA* expression, it significantly altered biofilm maturation, increased cell lysis and enhanced extracellular DNA release. Finally, by identifying three additional putative phosphatases that are capable of promoting sugar-phosphate tolerance, we show that *S. mutans* is capable of mounting a sugar-phosphate stress response by modulating the levels of certain glycolytic intermediates, functions that are interconnected with the ability of the organism to manifest key virulence behaviors.

Importance

Streptococcus mutans is a major etiologic agent for dental caries, primarily due to its ability to form biofilms on tooth surface and to convert carbohydrates into organic acids. We have discovered a two-gene operon in *S. mutans* that regulates fructose metabolism by controlling the levels of fructose-1-phosphate, a potential signaling compound that affects bacterial behaviors. With fructose becoming increasingly common and abundant in the human diet, we reveal the ways fructose may alter bacterial development, stress tolerance, and microbial ecology in the oral cavity to promote oral diseases.

Introduction

Most bacteria use the sugar:phosphotransferase system (PTS) to internalize mono- and di-saccharides, a process that uses phosphoenolpyruvate (PEP) to energize the transport and concomitant phosphorylation of the carbohydrates (1). While certain components of the PTS are vital to the growth and persistence of many bacteria, the accumulation in cells of phosphorylated carbohydrates can lead to sugar-phosphate stress, a condition that often manifests in growth inhibition or cell death (2-4). A number of mechanisms have been proposed to contribute to sugar-phosphate stress: (i) futile cycling, in which the cells expend energy to internalize and phosphorylate the sugar, but the sugar is then dephosphorylated and expelled (5); (ii) reduction of essential metabolic intermediates arising from an inability to internalize other carbohydrates (6); (iii)

creation of toxic metabolic byproducts, such as methylglyoxal (7, 8), or (iv) deleterious effects of specific sugar phosphates that act as allosteric modifiers of enzymes or regulatory proteins, causing dysregulation of metabolism (9). The majority of research on sugar-phosphate stress has been conducted with Gram-negative, model organisms, with far fewer studies carried out with known pathogens or Gram-positive bacteria (10).

Streptococcus mutans, a primary dental caries pathogen, is a Gram-positive, lactic acid-producing bacterium that depends on, and is particular adept at, transporting and fermenting carbohydrates for energy production and growth. The most studied sugar-phosphate stress in *S. mutans* is that induced by xylitol, a non-metabolizable pentitol that is internalized as xylitol-5-phosphate (X-5-P) by a fructose-specific PTS, but is subsequently dephosphorylated and released from the cells (11-13). Although the exact nature of the process remains to be clarified, including the enzyme(s) responsible for removing the phosphate group from X-5-P, it is generally believed that both the futile cycling of xylitol and the presence of X-5-P in cells are detrimental. While futile cycling wastes energy, it has been proposed that X-5-P is an inhibitor of phosphofructokinase that causes a block in glycolysis (9). The observed effects of xylitol intake by *S. mutans* include reductions in high-energy metabolites, such as fructose-1,6-bisphosphate (F-1,6-bP) and glucose-6-phosphate (G-6-P), as well as impaired glucose-PTS activity, decreased rates of acid production (14), and inhibition of the formation of extracellular insoluble polysaccharides from sucrose (15, 16). Given its ability to negatively affect a caries pathogen, xylitol is widely used as a non- or anti-

88 cariogenic additive in products that include chewing gum and candies, despite
89 the fact that spontaneous emergence of xylitol-resistant mutants can occur in
90 habitual users of xylitol-containing products (17, 18). It has been shown that the
91 fructose-PTS permease encoded by the *fruI* gene is responsible for transporting
92 the majority of xylitol, and a *fruI*-deficient mutant lost sensitivity to presence of
93 xylitol (18). Another example of sugar-phosphate-related stress in *S. mutans* is
94 one induced by 2-deoxyglucose (2-DG), an analog of glucose that can be
95 internalized and phosphorylated by the PTS, but cannot be metabolized. Uptake
96 of 2-DG by *S. mutans* reduces the transport of carbohydrates via the PTS (19)
97 and the multiple sugar metabolism (*msm*) system, an ATP-binding cassette
98 (ABC) transporter for melibiose, raffinose, and certain other carbohydrates that
99 are found in the human diet (20).
100 Fructose is transported into *S. mutans* via multiple PTS permeases and further
101 metabolism requires phosphofructokinase enzymes, including a 1-
102 phosphofructokinase and 6-phosphofructokinase that convert fructose-1-
103 phosphate (F-1-P) and fructose-6-phosphate (F-6-P), respectively, into F-1,6-bP
104 that can be further catabolized via glycolysis (3). We recently engineered a point
105 mutant in *S. mutans* strain UA159 (*fruK*M28stop, strain FruK-13) that prevents
106 the translation of an intact 1-phosphofructokinase (FruK) enzyme (3). Due
107 apparently to the accumulation of F-1-P in FruK-13, a severe growth phenotype
108 is evident when fructose is present. FruK-13 also displayed significant growth
109 defects when cultured in media containing glucose, sucrose, mannose,
110 galactose, lactose or certain amino sugars, demonstrated a broad influence of F-

1-P on carbohydrate metabolism and growth of *S. mutans* (3). RNA deep sequencing (RNA-Seq) was used to define changes in the transcriptome arising from loss of the FruK enzyme. The expression of 394 genes, including genes encoding ribosomal proteins, proteins required for biosynthesis of nucleotides and amino acids, and components of the PTS, were altered in FruK-13 compared to the parental strain (3). Among the most up-regulated genes in the *fruK* mutant were two open reading frames (ORF) in an apparent operonic arrangement, SMU.507 and SMU.508; designated *sppR* and *sppA*, respectively. SppR is a DeoR-type transcription regulator and SppA is a predicted hydrolase of the HAD (haloacid dehalogenase) family IIB that includes enzymes such as trehalose-6-phosphatase, plant and cyanobacterial sucrose-phosphatases, and a large subfamily of bacterial Cof-like hydrolases; Cof being an *E. coli* phosphatase. While both *sppR* and *sppA* are well conserved in *S. mutans* strains, homologous systems comprised of both genes in tandem have only been identified in *Streptococcus gordonii* and *Streptococcus sanguinis.* In this communication, we investigated the regulation and function of the *sppRA* operon and explored the contribution of its gene products to fitness and cariogenic potential of *S. mutans*, particularly in the context of regulation of F-1-P levels.

Results

Overexpression of *sppA* enhances growth of FruK-13 in the presence of fructose. In a previous study with a mutant lacking a 1-phosphofructokinase (*fruK*), FruK-13, an operon encoding a DeoR-like regulator (SMU.507, *sppR*) and

a predicted hydrolase of the HAD superfamily (SMU.508, *sppA*) was significantly up-regulated (3). As FruK-13 displays the most severe growth defect on fructose, likely due to accumulation of F-1-P, it was posited that certain enzymes encoded by *S. mutans* could eliminate these potentially toxic intermediates. The putative sugar-phosphate phosphatase encoded by *sppA* was cloned into an expression vector pIB184 behind a constitutive promoter and the resultant plasmid, pIB508, was introduced into FruK-13. After confirming enhanced expression of *sppA* by plasmid pIB508 (Fig. 1A), these resultant strains were compared in their growth phenotypes in a fructose-based medium. Compared to the vector-only control strain FruK-13/pIB184, which grew poorly on a TV-fructose medium, FruK-13/pIB508 grew at a rate comparable to the wild-type strain UA159 (Fig. 1B), providing a strong support for the hypothesis that SppA could function as a sugar-phosphate phosphatase that decreased the levels of F-1-P in the *fruK* genetic background.

SppA has hexose-phosphate phosphohydrolase activity. Multiple computer algorithms predicted that SppA is a hydrolase of the HAD superfamily. To study the function of SppA *in vitro*, the coding sequence of *sppA* was cloned into pQE30 and expression was induced in *E. coli* to produce an N-terminally His-tagged recombinant protein, designated His-SppA. His-SppA has 274 amino acids, excluding the His-tag, and migrated as a single 37-kDa band in SDS-polyacrylamide gel electrophoresis (SDS-PAGE). The protein was relatively stable in a variety of buffers and pH values, although addition of 0.5 M NaCl and

at least 10% of glycerol was required to retain activity during longer-term storage (>1 month) at 4°C. To test the kinetics of SppA in removing the phosphate group from presumptive substrates, a set of phosphate-free buffers were tested to carry out these experiments (see Materials and Methods for detail), and the phosphate released in each reaction was monitored using a Malachite green reagent kit.

Substrate specificity. Using 2.5 mM *p*-nitrophenylphosphate (*p*NPP) as a general colorimetric substrate for phosphatases, phosphatase activity by His-SppA was detected at 37°C in 50 mM HEPES buffer at pH 7.5. SppA activity on *p*NPP could be stimulated by the addition of millimolar concentrations of $MgCl_2$ (data not shown). We then conducted a number of preliminary experiments to gain insights into optimal conditions for activity of His-SppA on a number of sugar phosphates. Then, as determined by an end-point assay performed under optimized conditions (Fig. 2A), the preferred substrate for His-SppA was found to be F-1-P, followed by F-6-P. Very little activity was observed when F-1,6-bP, G-6-P, or GlcN-6-P were used as substrates, and SppA had no activity on GlcNAc-6-P under the conditions tested.

Effects of metal ions. Many phosphatases are affected by the presence of metal ions (21), thus the activity of His-SppA was studied by adding to the reactions millimolar levels of $CaCl_2$, $CuSO_4$, $MgCl_2$, $MnCl_2$, and $ZnCl_2$. $CaCl_2$, $CuSO_4$, and $ZnCl_2$ at these levels had no detectable impact to the activity of His-SppA on F-1-P as a substrate, but the presence of $MgCl_2$ and $MnCl_2$ significantly enhanced the release of phosphate by the purified, recombinant enzyme (Fig. 2). By testing both Mg^{2+} and Mn^{2+} together, it was determined that optimal enzymatic

activities could be elicited when $MgCl_2$ was present at 5 mM, along with 1 mM $MnCl_2$.

pH. The optimal pH for the activities of His-SppA was determined to be about 6.5, and the rate of phosphate release significantly decreased when the pH values of the reaction deviated from this point, particularly at values of 6.0 and below (Fig. 2C). Since *S. mutans* maintains ΔpH values of 0.5 to 1.0 units above the external environment (22), SppA is probably most active in cells growing in a moderately acidic environment, such as what would occur when *S. mutans* is actively metabolizing carbohydrate(s).

Fluoride. Sodium fluoride (NaF) is an inhibitor of many phosphatases. The presence of 10 mM NaF significantly reduced (by >50%) the rate of phosphate release from F-1-P by His-SppA (Fig. S1 in the supplemental material).

Reaction kinetics on F-1-P and F-6-P. Finally, using the optimal pH and metal ion conditions described above, V_{max} and K_m of His-SppA were measured using F-1-P or F-6-P. The purified enzyme was incubated with increasing concentrations of each substrate (see Materials and Methods for details) at 37°C, and release of phosphate over time was monitored by periodic sampling of the reactions. The release rate of phosphate for each reaction was then plotted against the substrate levels to estimate rate and substrate affinity (Fig. 2D). For F-1-P, the V_{max} was 9.50 ± 0.38 µmol/(min x mg protein), and the K_m was 1.90 ± 0.21 mM. For F-6-P, the V_{max} was 0.52 ± 0.03 µmol/(min x mg protein) and the K_m was 4.83 ± 0.51 mM. Thus, under these conditions, F-1-P is a preferred substrate for SppA, whereas F-6-P can be dephosphorylated by SppA, albeit less

efficiently. These data are consistent with idea that *S. mutans* may use SppA to limit accumulation of F-1-P, which can be further phosphorylated (by FruK) into F-1,6-bP. However, the data may also reflect a preference of the organism to internalize then further metabolize F-6-P. These parameters, including V_{max} and $K_{m,}$ are also in line with what has been reported for other members of the HAD family phosphatases in bacteria (5, 23, 24).

SppR is a negative regulator of *sppA* that responds to fructose-phosphate signals. SppR is predicted to be a member of the DeoR family, a group of transcription regulators that often respond allosterically to metabolic intermediates including phosphorylated carbohydrates. To begin understanding the mode of regulation by SppR, a deletion mutant of *sppR* was constructed and the expression of *sppA* was measured using quantitative RT-PCR (qRT-PCR). The results showed a significant enhancement (8.95-fold ± 1.03-fold) in mRNA levels of *sppA* due to the loss of SppR, when both the wild type and the mutant were growing in the rich medium BHI.

Since higher expression of both *sppR* and *sppA* was noted using RNA-Seq of the *fruK* mutant (FruK-13), which should have elevated levels of F-1-P, it was hypothesized that SppR negatively regulates the *spp* operon, with SppR being allosterically regulated by fructose phosphates, including F-1-P. To test this hypothesis, the promoter activity of the operon (P*sppR*) was examined by utilizing a promoter-reporter gene fusion P*sppR::cat* that was integrated in single copy at a distant site on the chromosome. Expression of the *cat* fusion was

measured in cells growing on various carbohydrates. A UA159 derivative carrying the P*sppR::cat* fusion was cultivated in TV medium supplemented with 10 mM glucose to mid-exponential phase, then pulsed for 1 h with 25 mM or 50 mM fructose to increase the levels of fructose-derived metabolites. In addition, 25 mM or 50 mM of glucose, xylitol, or sucrose were also used to treat these cells. The CAT activities measured (Fig. 3A) on cells pulsed with fructose showed significant, concentration-dependent increases compared to cells pulsed with glucose. A slight reduction in CAT activity was noted in cells pulsed with 50 mM xylitol, and sucrose had little to no impact on the expression of the *spp* promoter fusion. When compared to glucose, treatment of cells with fructose should result in accumulation of F-1-P, adding support to the idea that F-1-P is an allosteric effector capable of relieving the repression by SppR. On the other hand, xylitol treatment could potentially reduce the capacity of the PTS and carbon flux, reducing the levels of glycolytic metabolites, including F-1-P and F-6-P. The lack of response from sucrose treatment could be due to the preference by the bacterium to utilize the glucose moiety, as our recent study has indicated that free fructose is expelled by *S. mutans* after sucrose is transported and phosphorylated on the glucose moiety by ScrA, and the resultant sucrose-6-phosphate (S-6-P) is cleaved by ScrB (25).

We have previously shown that fructose internalization via FruI likely results in creation of F-1-P, whereas internalization of fructose by EII^{Lev} (*levDEFG*) yields F-6-P (3). To test if transport of substrates via different PTS permeases could affect the regulation of expression of the *spp* operon, the P*sppR::cat* fusion was

placed in the background of mutants deficient in the fructose-PTS permeases, *levD* or *fruI*, or in a mutant lacking the primary glucose-PTS permease (*manL*) (26). A mutant defective in production of catabolite control protein A (CcpA), a major regulator of genes involved in carbon flow in *S. mutans*, was also included as CcpA can regulate the expression of certain PTS permease genes (27). The wild-type control and the mutant strains were grown in TV-glucose to mid-exponential phase, then pulsed with 50 mM fructose to induce the P*sppR::cat* fusion. In support of our hypothesis that F-1-P is required for inducing expression of *spp*, loss of *fruI* abolished fructose-dependent induction of CAT activity, whereas the *levD* mutant behaved like the wild type (Fig. 3B). Interestingly, a deletion of the glucose-PTS gene *manL* resulted in significantly increased expression of the P*sppR::cat* fusion, consistent with our recent study that showed interconnected regulation of fructose and glucose PTS permeases in *S. mutans* (3). The *ccpA* mutant showed no difference in response to fructose.

To gauge the overall impact of the regulation by SppR on the *sppRA* operon and the potential that depletion of F-1-P associated with *sppA* induction could function in feedback regulation of the operon, we assayed the expression of P*sppR::cat* fusion in strains deficient in *sppR* and *sppA*, respectively. The results (Fig. 3B) showed nearly a 2-log increase in CAT activities in the *sppR* mutant regardless of the sugars tested, and no change in the *sppA* mutant. Together, these results suggest that SppR exerts a strong, negative regulation over the *spp* operon, resulting in low levels of expression of *sppA* even when fructose is present, at least in an otherwise wild-type genetic background.

SppR binds to the *spp* promoter and to F-6-P. To demonstrate the direct interaction of SppR with its own promoter region, a recombinant His-SppR was engineered and overexpressed in *E. coli*. The purified His-SppR was used in an electrophoretic mobility shift assay (EMSA) that included a biotin-labeled DNA fragment containing the 250-bp intergenic region immediately upstream of the *sppR* coding sequence. As shown in Fig. 4A, the presence of 0.5 µM His-SppR resulted in significant shifting of the DNA probe. However, when the reaction was repeated with the addition of 5 mM sugar-phosphates, including F-1-P, F-6-P, F-1,6-bP and G-6-P, there was little effect on the interactions of His-SppR with the probe.

As an alternative to EMSA, we also performed a thermal shift assay in which increasing temperature induces unfolding of His-SppR, which is monitored using a protein dye that fluoresces when bound to unfolded polypeptides (28). The melting temperature (Tm) of proteins usually increases in the presence of compounds that are bound by the protein. We added to the melting reaction various amounts of glucose, G-6-P, fructose, F-1-P, F-6-P, F-1,6-bP, GlcN, GlcN-6-P, GlcNAc and GlcNAc-6-P. While most sugar and sugar phosphates had no impact to the unfolding of His-SppR, addition of F-6-P increased the Tm in a dose-responsive manner, indicating an interaction between F-6-P and His-SppR. By plotting the Tm values of the reactions against the concentrations of F-6-P used, it was determined that F-6-P associates with His-SppR with a *Kd* of 3.6 ± 0.15 mM (Fig. 4B). Considering the results of our genetic analysis, we posit that

295 the interactions between SppR and fructose-derived metabolites modulate the
296 repression of *spp* expression. It is not clear why F-1-P did not elicit an increase in
297 Tm in this system. In the future, we plan to utilize a spectrum of binding assays
298 and non-tagged SppR proteins to further evaluate the possible allosteric effectors
299 that modulate the DNA-binding affinity of SppR *in vivo.*
300
301 **Overexpression of SppA enhances resistance to xylitol.** Having
302 demonstrated that enhanced expression of SppA from pIB508 abolished the
303 sugar-phosphate stress in strain FruK-13, we tested if overexpression of SppA
304 could also alleviate stress caused by the presence of xylitol. Strains
305 UA159/pIB184 and UA159/pIB508 were created and their growth was monitored
306 in TV containing 0.5% glucose or fructose, with or without 1% xylitol. Without
307 addition of xylitol, both strains grew similarly well in TV glucose or fructose (data
308 not shown). When 1% xylitol was added to the TV-glucose medium,
309 UA159/pIB184 displayed a reduced growth rate compared to when the strain was
310 grown in TV with glucose alone. Interestingly, UA159/pIB508 showed
311 significantly faster growth than UA159/pIB184 in the presence of both glucose
312 and xylitol, indicating enhanced resistance to xylitol as a result of increased
313 expression of SppA (Fig. 5A; see Fig. 1A for *sppA* mRNA levels). In contrast,
314 addition of 1% xylitol to TV-fructose had no discernable effect on the growth
315 phenotypes of either strain (data not shown); a result consistent with the notion
316 that xylitol is internalized via a fructose-specific PTS (FruI) (18). In this case, our

interpretation is that fructose competes better than xylitol for uptake, so less xylitol is internalized and there is less of an impact on growth.

Since deletion of *sppR* enhanced the expression of *sppA* (Fig. 3B), we compared resistance to xylitol by the wild type and its otherwise-isogenic *sppR* and *sppA* mutants. The *sppR* mutant showed significantly improved growth in TV-glucose supplemented with 1% of xylitol, similar to UA159/pIB508 that overexpressed *sppA* (Fig. 5B). However, loss of *sppA* had no effect on xylitol resistance, as the *sppA* mutant grew similarly to the wild type. These results agree with our earlier findings that the expression of *sppA* is likely maintained at minimal levels, perhaps to avoid futile cycling. We have attempted, but have failed, to demonstrate the capacity of SppA to dephosphorylate xylitol-5-phosphate (X-5-P)(see Text S1 in the supplemental material), in large part due to the difficulty producing sufficient amounts of the compound; it is not commercially available.

Accumulation of F-1-P enhances eDNA release and affects biofilm formation. *S. mutans* depends on the development of biofilms for its virulence, but little information is available on the effects of fructose on *S. mutans* biofilms. Wild-type cultures in exponential phase were grown in BHI and used to inoculate a biofilm medium (BM) constituted with 2 mM sucrose and 18 mM glucose (BMGS) or 18 mM fructose (BMFS), as well as a number of combinations of both glucose and fructose totaling 18 mM hexose. After 24 h or 48 h of incubation, the supernates of the culture were removed and development of biofilms was

visualized and quantified by staining with 0.1% crystal violet. As shown in Fig. 6A, growth on fructose (BMFS) changed the accumulation of biomass by *S. mutans* on a polystyrene surface, resulting in a thinner but more uniform biofilm, as opposed to a patchy coverage by the biofilms formed on BMGS. Elution of crystal violet also indicated that greater amounts of dye were retained by the biofilms formed on fructose than glucose (Fig. 6A). This effect was not likely a result of reduced growth caused by a lack of glucose, as similar phenotypes were visible by the presence of as little as 3 mM fructose (data not shown). Also, to differentiate between effects of internalization of F-1-P versus F-6-P, we included the otherwise-isogenic mutants of UA159 deficient in either *fruI* (F-1-P) or *levD* (F-6-P). The results (Fig. 6A) showed that while the wild type and both mutants formed similar biofilms in BMGS, the *fruI* mutant formed patchy biofilms on BMFS, resembling those on BMGS. The *levD* mutant behaved like the wild type.

Recent research has suggested that the ability of *S. mutans* to form efficient biofilms depends on both the synthesis of glucans and the release of extracellular DNA (eDNA) by bacteria, via both lysis-dependent and -independent pathways (29). To further study the effects of fructose, the release of eDNA was quantified using a fluorescent DNA dye in the biofilms of *S. mutans*. The results were normalized against the viable counts of bacteria (CFU). When grown as biofilms in BMFS, UA159 released significantly more eDNA per CFU after 24 h (5-fold) or 48 h (17-fold) of growth compared to BMGS medium (similar to UA159/pIB184 in Fig. 6C). Significantly lower CFU (5-fold for 24 h, and 20-fold for 48 h) were recovered from biofilms formed on BMFS than BMGS. As such,

363 the amounts of eDNA detected per unit volume of supernatant fluid were
364 comparable for both BMGS and BMFS. Therefore, it appears that the bacteria
365 incubated in the presence of fructose experienced significantly more lysis, which
366 resulted in increased release of eDNA and changes in formation of biofilms;
367 although at this point we cannot rule out the involvement of other routes for
368 production of eDNA. When treated with a LIVE/DEAD stain and observed under
369 a confocal laser-scanning microscope, the biofilms formed on BMFS indeed
370 showed notably more dead cells than those formed on BMGS (Fig. 6B). Similar
371 impacts of fructose were observed for biofilm development by other genomically
372 distinct, wild-type isolates of *S. mutans* (30), so the phenomenon is not restricted
373 to the lab strain UA159 (Fig. S2 in the supplemental material). Furthermore, we
374 compared the sensitivity of planktonic *S. mutans* cells to the cell wall-degrading
375 enzymes lysozyme and mutanolysin by extracting chromosomal DNA after
376 enzymatic treatment, using batch cultures grown in glucose- or fructose-
377 containing medium. The results showed that 10-fold more DNA could be
378 harvested from UA159 that was cultured in TV-fructose, compared to cells
379 cultivated in TV-glucose, after each was treated with lysozyme, or a combination
380 of lysozyme and mutanolysin, under otherwise-identical conditions (Fig. S3 in the
381 supplemental material).
382 As a further test of our hypothesis that F-1-P in particular is responsible for the
383 fructose effects observed so far, the strains UA159/pIB508 and UA159/pIB184
384 were compared in their ability to produce eDNA in the 48-h biofilm model. Similar
385 to UA159, strain UA159/pIB184 yielded significantly lower numbers of CFU, but

much higher levels of eDNA/CFU when growing on BMFS compared BMGS (Fig. 6C). When *sppA* was overexpressed on pIB508, significant reductions in the release of eDNA/CFU were apparent in comparison to strain UA159/pIB184, an impact that was especially significant for cells cultured in BMFS. At the same time, bacterial viable counts also showed significant recovery as an effect of pIB508, particularly when assayed using BMFS (Fig. 6D). These results suggest that accumulation of F-1-P in *S. mutans* likely leads to alterations in the cell-envelope that results in enhanced autolysis and release of eDNA, causing aberrant biofilm phenotypes.

Other putative phosphatases capable of promoting sugar-phosphate resistance. The existence in *S. mutans* of a xylitol-inducible phosphatase capable of dephosphorylating X-5-P has been proposed (31). As xylitol reduced *spp* expression (Fig. 3A), we hypothesized that other phosphatase(s) are produced that may act on xylitol. Based on sequence similarity to SppA and other bacterial sugar-phosphate phosphatases, a functional genomics approach was employed to identify genes encoding products that could promote resistance to xylitol. A total of 9 ORFs were selected and mutated by allelic exchange with an antibiotic resistance marker, and three (SMU.428, SMU.488 and SMU.718c) were chosen as potential candidates based on the decreased growth rates (Fig. S4 in the supplemental material) and yields (Fig. 7A) of the mutants in the presence of xylitol, compared to the wild type. For confirmation, these genes were expressed constitutively using pIB184, in both the wild-type and the

respective mutant genetic backgrounds. When assayed for growth on TV-glucose supplemented with xylitol, mutants that were complemented by each of these three genes regained resistance to xylitol, and UA159 containing SMU.718c or SMU.488 expressed from pIB184 also showed enhanced yields, compared to their respective vector-only controls (Fig. S5 in the supplemental material). Furthermore, we previously reported that a deletion of the tagatose-1,6-bisphosphate aldolase (LacD) results in sensitivity to galactose in *S. mutans,* likely due to accumulation of metabolic intermediates that are normally catabolized by the tagatose pathway (32). When pIB428 was introduced into the *lacD* mutant, there was a significant alleviation of the inhibitory effects of galactose (Fig. 7B). We found that SMU.428, SMU.488 and SMU.718c are well conserved in the genomes of a diverse group of *S. mutans* isolates (30). Amino acid sequence alignments performed using these three proteins, together with SppA and the AphA phosphatase from *E. coli* (33), showed significant conservation in those amino acid residues (Fig. S6 in the supplemental material) that place these proteins in the family of bacterial class B acid phosphatases, part of the DDDD superfamily of phosphohydrolases (34). Computer analysis failed to identify any potential signal peptide sequences in the N-terminus of these proteins, suggesting they are not secreted. Further research is needed to understand their contribution to xylitol resistance and more broadly, to sugar-phosphate stress.

Discussion

Carbohydrate fermentation is a highly dynamic process where the relative activities of various enzymes and resultant intermediates must be maintained at optimal levels to ensure fitness and survival, and to balance anabolic and catabolic processes. Perturbations to the systems, such as those that occur in the oral microbiome during intake of dietary carbohydrates by the host, require rapid responses by the microbiota. Sugar-related stress responses mediated by complex regulatory systems have been characterized mostly in Gram-negative model bacteria, e.g., *E. coli* (8, 35, 36). As a major caries pathogen, *S. mutans* depends on carbohydrate fermentation for energy generation and virulence. *S. mutans* is particularly well adapted to metabolizing sucrose, in part through the activities of three secreted glucosyltransferases (GtfB, GtfC and GtfD) that convert sucrose into glucan polysaccharides that serve as the scaffolding for biofilm accumulation and in creation of a diffusion-limiting matrix (37). Interestingly, Gtfs generate a molecule of free fructose for every glucose moiety of sucrose that is targeted toward glucan formation. Furthermore, it is now clear that the majority of the sucrose presented to *S. mutans* is internalized by a sucrose-specific PTS permease (38). After internalization and phosphorylation, sucrose is cleaved by a sucrose-6-phosphate hydrolase into G-6-P and fructose. However, a significant portion of the fructose thus generated is expelled into the environment and re-internalized by fructose PTS permeases (25, 39). These observations, when coupled with the fact that fructose itself is a major constituent of foodstuffs, e.g. with high-fructose corn syrups increasingly used as common

455 sweeteners, necessitate a better understanding of the metabolism of fructose by
456 the oral microbiome.
457 *S. mutans* maintains at least three PTS permease operons (*fruRKI*, *fruPCD*
458 and *levDEFG*) plus three phosphofructokinases (FruK, FruP, and
459 SMU.1191/Pfk). Further, while a number of *S. mutans* PTS permeases can
460 transport sugars other than their primary cognate carbohydrate, there are no
461 other instances in *S. mutans* of redundancy in PTS permeases for sugars,
462 besides those for fructose. This redundancy in PTS permeases, in itself, is
463 noteworthy and could reflect significant evolutionary benefits to redundant
464 fructose catabolic systems. Much remains to be clarified regarding the
465 contributions of these PTS operons to the establishment and persistence of *S.*
466 *mutans* in the human oral cavity, and to the organism's cariogenic potential.
467 However, it is understood that both F-1-P and F-6-P generated by the PTS are
468 further phosphorylated to create F-1,6-bP, likely via 1-phosphofructokinase FruK
469 and 6-phosphofructokinase SMU.1191, respectively. F-1,6-bP is then cleaved by
470 an F-1,6-bP-specfic aldolase into glyceraldehyde 3-phosphate and
471 dihydroxyacetone phosphate (3). We have demonstrated that removal of FruK
472 leads to significant growth and fitness defects in *S. mutans*, apparently due to
473 accumulation of the metabolic intermediate F-1-P (3). Here we present evidence
474 that *S. mutans* maintains tight control over the levels of F-1-P through an
475 inducible sugar-phosphate phosphatase (*spp*) operon, consisting of a
476 transcriptional regulator SppR and a fructose-phosphate hydrolase SppA.
477 Changes in F-1-P levels, either increase or decrease, significantly alter bacterial

478 physiology, including cell envelope integrity and biofilm development. We
479 hypothesize that, aside from being an apparent stress compound in *S. mutans*
480 (6), that F-1-P may also act as a signaling molecule, the accumulation of which
481 promotes autolysis and release of extracellular DNA; with the latter being a
482 critical contributor to formation of biofilms (29).

483 In support of this hypothesis, our latest RNA deep sequencing analysis in *S.*
484 *mutans* has identified a fructose regulon that includes a significant number of
485 genes that are likely involved in stress responses (25). For example, growth on
486 fructose up-regulated the *cid* operon (SMU.1700c~1703c) that influences
487 oxidative stress resistance and modulation of autolysis and biofilm development
488 (40). Also up-regulated were the *rcrRPQ* and *relPRS* operons (SMU.921 to
489 SMU.928) which have major impacts on acid and oxidative stress tolerance,
490 competence development and (p)ppGpp metabolism (41). Thus, fructose and its
491 intermediates are directly linked to pathways that are critical for persistence,
492 growth and survival decisions, nutrient acquisition and genetic diversification.

493 On the other hand, a growing body of evidence suggests that F-1-P is acting
494 as a regulatory molecule for *S. mutans*. Our recent study on the function of the
495 *fruRKI* operon has detailed the transcriptomic impact of accumulation of F-1-P, a
496 compound that likely serves as an allosteric effector to another DeoR-type
497 regulator, FruR (3). It was clear that F-1-P influences gene regulation beyond the
498 *fruRKI* operon. Specifically, the *fruK* mutant showed altered expression in as
499 many as 20 known or probable transcriptional regulators, impacting ~20% of the
500 genome. Key functions ranging from energy metabolism, protein and nucleic acid

biosynthesis, to stress tolerance were affected by fructose. In addition to showing that overproduction of SppA, which preferentially degrades F-1-P, leads to phenotypic changes in both xylitol resistance and eDNA release, we have shown that the ability of fructose to induce *spp* operon expression depends on an intact FruI protein, which encodes the fructose-PTS permease that creates F-1-P (3). The lack of interactions between F-1-P and the recombinant SppR protein *in vitro* could suggest the requirement for other factors in addition to F-1-P that influence SppR activity or the contribution of other regulatory proteins. Conversely, addition of the His-tag to SppR altered the F-1-P binding behavior of the recombinant protein, compared to native SppR. The interaction of SppR with F-6-P that we observed *in vitro* also points to further complexity in this system. For example, F-6-P could act as a second allosteric effector for SppR, perhaps when present at high concentrations. Future research will focus on identifying other regulatory circuits that respond to the accumulation of F-1-P, both directly and indirectly, in particular the pathway(s) responsible for cell envelope integrity and biofilm phenotypes. As stated earlier, the *spp* operon has only been identified in a few oral streptococcal species, and its specificity for F-1-P could have implications in understanding niche adaptations and oral microbial ecology.

An intracellular hexose-6-phosphate: phosphohydrolase was purified from *Lactococcus lactis* that has a preference for galactose-6-phosphate and F-6-P (23). This enzyme had an estimated M_r of 60 KDa by SDS-PAGE, was most active at pH 6.0, and its activity was stimulated by Mn^{2+}, Mg^{2+} and Fe^{2+}, and inhibited by fluoride. Another bacterial sugar phosphate phosphatase, Spp, was

524 recently identified in *Pseudomonas fluorescens* that was capable of
525 dephosphorylating ribose-5-P, F-6-P, and G-6-P (5). The optimal Mg^{2+}
526 concentration for Spp was determined to be 2.5 mM, whereas addition of Mn^{2+}
527 reduced the reaction rate. Therefore, SppA appears to share some similarities
528 with other bacterial phosphohydrolases, yet it stands out with its preference for F-
529 1-P. Lastly, despite our repeated efforts, we were not able to determine whether
530 X-5-P is a substrate of SppA, partly due to our inability to obtain or generate
531 sufficient X-5-P (it is not commercially available). As we continue to resolve this
532 technical issue, it is important to note the possibility that SppA alleviates xylitol-
533 related stress through its activities on either F-1-P or F-6-P, as X-5-P has been
534 suggested to inhibit the activities of phosphofructokinases (9). The same
535 rationale could apply in interpreting the xylitol phenotypes associated with the
536 mutants that lacked one of three additional HAD phosphatases; that each
537 enzyme may have multiple substrates and a stress phenotype could be alleviated
538 by actions on molecules other than the one triggering the stress. Most notably,
539 overexpression of SMU.428 abolished galactose-mediated stress in a *lacD*
540 mutant. SMU.428 is located immediately downstream of the *copYAZ* operon that
541 is responsible for copper efflux, biofilm formation and stress tolerance, yet its
542 homologues in a number of other streptococci are closely associated with the
543 tagatose operon. Clearly though, *S. mutans* possesses multiple
544 phosphohydrolases and related regulatory proteins capable of mounting a stress
545 response when triggered by certain sugar-phosphates. Additional research is

needed to understand the function and regulation of these putative sugar-phosphate phosphatases.

Materials and Methods

Bacterial strains and culture conditions. *Streptococcus mutans* strains (Table 1) were maintained using brain heart infusion (BHI)(Difco Laboratories, Detroit, MI) agar plates or in liquid BHI medium at 37°C, in an aerobic atmosphere supplemented with 5% CO_2. To monitor bacterial growth phenotypes and for most other experiments, a semi-synthetic Tryptone-vitamin (TV) medium (42) was utilized with various carbohydrates being provided at specified concentrations. Overnight bacterial cultures were prepared in BHI, then sub-cultured to exponential phase, and inoculated at 1:100 dilutions into TV media. Growth was monitored as the change in optical density at 600 nm (OD_{600}) using a Bioscreen C lab system (Labsystems Oy, Helsinki, Finland). For development of biofilms in 96-well polystyrene plates or ibidi glass chambers (ibidi GmbH, Martinsried, Germany), a biofilm medium (BM)(43) was utilized that contained 2 mM sucrose and varying amounts of glucose or fructose, with bacterial inoculum prepared in BHI. Each of these experiments was repeated at least three times using independent cultures (biological replicates), with each sample being represented by at least two wells (technical replicates).

DNA methodology. Standard recombinant DNA techniques were employed in preparation of genetic materials for applications such as cloning and

569 mutagenesis (44). To engineer a mutant defective in *sppR*, a set of 4 primers
570 (Table 2) were designed for PCR amplification of two DNA fragments flanking the
571 coding sequence of *sppR* (upstream fragment: SMU.507-1 and SMU.507-2GA;
572 downstream fragment: SMU.507-3GA and SMU.507-4). PCR reactions were
573 carried out using these primers to generate two DNA fragments that shared >25
574 bp overlaps with the 5'- and 3'- ends, respectively, of a kanamycin-resistance
575 cassette. Subsequently, these flanking DNA fragments were used in equimolar
576 concentrations, together with the kanamycin cassette, in a one-step ligation
577 reaction that was catalyzed by a Gibson assembly kit (New England Biolabs,
578 Beverly, MA). The ligated product was then used to transform a naturally
579 competent UA159 culture, followed by selection on BHI agar plates containing
580 kanamycin (1 mg/ml). Similar procedures were carried out in the creation of
581 mutants defective in *sppA*, SMU.428, SMU.488, SMU.718c and other genes. All
582 strains created in this study have been validated by DNA sequencing to ensure
583 that no unintended mutations were introduced into the flanking regions of the
584 gene of interest.
585 To construct a complementing plasmid for the *sppA* mutant, a pair of primers
586 (SMU.508-5'Bm and SMU.508-3'SacI) were designed and used for amplification
587 of the coding sequence of *sppA,* together with its putative ribosome-binding site.
588 This DNA product was treated with restriction enzymes *Bam*HI and *Sac*I, and
589 then ligated with an expression vector pIB184 (45) that was linearized with the
590 same enzymes. After cloning into an *Escherichia coli* host strain BH10B, the
591 resultant plasmid pIB508 was verified to contain the desired coding and

regulatory sequences and introduced into the *sppA* mutant background, as well as the wild type UA159. Three additional plasmids, pIB428, pIB488, and pIB718c, were constructed in the same way, in the pIB184 vector, and used to complement their respective mutants. To monitor the transcriptional activities of the *spp* operon, a P*sppR::cat* fusion was constructed by cloning a DNA fragment containing the intergenic region upstream of *sppR* onto the integration vector pJL84 that contained a promoterless *cat* gene (46), and the gene fusion was subsequently delivered into a distal site on the chromosome of *S. mutans* by double cross-over recombination. The sequence information of all these primers is included in Table 2.

To assess the resistance of different UA159 cultures to muralytic enzymes, the bacteria were cultivated overnight in 5 ml TV medium containing 0.5% glucose or fructose, harvested by centrifugation at 4°C and washed once with a TE buffer (10 mM Tris-Cl, 1 mM EDTA, pH 8.0). Cells were resuspended in 500 µl of lysis buffer that contained 50 mM Tris-Cl at pH 8.0, 10 mM EDTA, 10 mg/ml of lysozyme, and 0.1 mg/ml of RNase A. After addition of 0 or 20 units of mutanolysin (from *Streptomyces globisporus,* Millipore Sigma, St. Louis, MO), cells were incubated at 37°C for 1 h, and lysed by adding 40 µl of 20% SDS and incubating at 80°C for 15 min. Subsequently, 80 µl of 5 M NaCl was added into each reaction, mixed well, followed by addition of 600 µl of phenol: chloroform: isoamyl alcohol (25: 24: 1, v/v/v) and 2 min of vortexing. The solution was then clarified by centrifugation at room temperature at 15000 × *g* for 5 min, followed by the removal of 500 µl of the aqueous phase. The genomic DNA was then

615 precipitated from the aqueous solution by addition of 500 µl 100% isopropanol
616 and centrifugation as before. After washing once with 75% ethanol, the DNA was
617 air-dried and dissolved in 50 µl TE buffer and quantified using a Nanodrop
618 apparatus (Thermo Fisher, Waltham, MA) and agarose-gel electrophoresis.
619
620 **Engineering and preparation of recombinant proteins of SppR and SppA.**
621 DNA fragments containing the entire coding sequences of SppR and SppA were
622 each amplified using PCR primers (SMU.507-5'Bm and SMU.507-3'HIII for *sppR*,
623 and SMU.508-5'Bm and SMU.508-3'HIII for *sppA*)(Table 2) containing
624 engineered restriction sites, and digested using restriction enzymes *Bam*HI and
625 *Hin*dIII. After ligating with a pQE30 vector prepared by treating with the same
626 enzymes to create an N-terminal, 6×His-tagged gene product, the constructs
627 were introduced into *E. coli* M15. After confirming the fidelity of the PCR and
628 cloning via DNA sequencing, the expression of each recombinant protein was
629 induced by adding IPTG to a final concentration of 0.05 mM to cells growing at
630 mid-exponential phase.
631 Purification of recombinant proteins, His-SppR and His-SppA, was carried out
632 using a Ni-NTA agarose according to protocols provided by the supplier
633 (Qiagen), with some modifications. Briefly, to improve the stability of His-SppR,
634 10% of glycerol was supplemented to each of the original lysis buffer (50 mM
635 NaH_2PO_4, 0.3 M NaCl, and 10 mM imidazole, pH 8.0), the wash buffer and
636 elution buffer. After elution from the column, His-SppR was dialyzed against a
637 buffer containing 10 mM HEPES pH 7.5, 0.5 M NaCl and 20% glycerol, using a

0.5-mL Slide-A-Lyzer dialysis device with a MWCO of 3.5 KDa (Thermo Fisher). To avoid carryover of phosphate into the subsequent reactions involving the recombinant SppA, purification of His-SppA was performed using a phosphate-free buffer system that was created by replacing the NaH_2PO_4 with 50 mM HEPES (pH 7.9), and also by supplementing with 10% glycerol. Dialysis of the purified His-SppA solution was carried out against 10 mM PIPES pH 6.5, 0.5 M NaCl, and 20% glycerol.

Electrophoretic mobility shift assay (EMSA) and thermal shift. To study the interaction of His-SppR with the promoter of *sppR*, EMSA was performed using a biotin-labeled DNA fragment containing the intergenic region upstream of the *sppR* coding sequence as previously described (47). When needed, the sugar phosphates were each used at 5 mM. To study the interaction of SppR with various sugar phosphates, a 10-µM His-SppR solution was prepared using a buffer containing 0.1 M HEPES (pH 7.5) and 0.15 M NaCl. After addition of a SYPRO Orange protein stain (Thermo Fisher), used at a 6000-fold dilution, and 5 mM of each sugar phosphate, the 10-µL reactions were subjected to a melting-curve treatment on a CFX96 Touch real-time PCR thermocycler (Bio-Rad, Hercules, CA) by increasing the temperature from 25°C to 75°C in increments of 0.2°C. The RFU measurements were then plotted against the temperature values to determine the melting temperature (Tm) (28).

Phosphatase assay. The ability of His-SppA to remove the phosphate group from various sugar-phosphates was measured at 37°C. The basic buffer was composed of 50 mM PIPES pH 6.5, 5 mM $MgCl_2$, and 1 mM $MnCl_2$. For other pH values, different buffering reagents were used in place of PIPES at the same concentration: 2-ethanesulfonic acid (MES) or potassium citrate (K-Cit) for pH 5.5; 1,4-piperazinediethanesulfonic acid (PIPES) for pH 6.0 and pH 6.5; and HEPES for pH 7.0 and pH 7.5. All initial experiments to determine the effects of metal ions were carried out in an end-point assay at neutral pH.

To measure the reaction kinetics of His-SppA on F-1-P, 20 µL of His-SppA that was diluted to 1 µM using the dialysis buffer was mixed with 40 µL of F-1-P prepared in the basic buffer, at final concentrations ranging from 0.1 mM to 1.0 mM; for F-1-P ranging from 1.5 mM to 10 mM, 0.25 µM of protein was used. All components were pre-warmed to 37°C before mixing. With the reaction maintained at 37°C, a 5-µL aliquot of the reaction was removed at 1 min intervals and subjected to measurement of free phosphate using a phosphate assay kit (Malachite Green Reagent, MGR; Sigma). For the kinetics of His-SppA with F-6-P as a substrate, 20 µL of His-SppA at 2 µM was used in each reaction, and aliquots of the reaction were taken and measured every 5 min. Each reaction was repeated twice. The data were analyzed using the Prism from GraphPad software (La Jolla, CA).

Biofilm development, microscopy and measurement of extracellular DNA (eDNA). Development of biofilms by *S. mutans* was investigated in 96-well

683 polystyrene plates (Thermo Fisher) for comparison of overall biofilm mass, or on
684 glass surfaces using an ibidi 8-well μ-Slide to assess structural changes and
685 release of eDNA. A semi-defined biofilm medium (BM) was modified to contain
686 final concentrations of 2 mM sucrose and 18 mM glucose (BMGS) or fructose
687 (BMFS)(3, 48). Exponential-phase bacterial cultures prepared using BHI were
688 diluted 1:100 into BMGS or BMFS and incubated at 37°C in an aerobic
689 environment supplemented with 5% CO_2. Each experiment included at least
690 three biological replicates. The 96-well plates were incubated for 24 to 48 h,
691 washed with phosphate-buffered saline (PBS), and stained with 0.1% crystal
692 violet (CV). After extensive washing with water, the retained CV was eluted with
693 a solution of 30% acetic acid and quantified by measuring the optical density at
694 575 nm (OD_{575}).
695 The ibidi slides were incubated for 48 h, with a replacement of medium after
696 first 24 h. For observation of biofilm structures, each biofilm was treated using a
697 LIVE/DEAD BacLight bacterial vitality stain kit (Thermo Fisher) and visualized
698 using a confocal laser scanning microscopy system (4). To assess the amount of
699 eDNA released by each biofilm, the entirety of the 48-h biofilm culture was
700 harvested by scraping off the biofilm material, without washing, and sonicated for
701 30 sec at 100% power using a water-bath sonicator (model FB120, Thermo
702 Fisher). A portion of the cell suspension was subjected to serial dilutions and
703 plated on BHI plates for enumeration of CFU, and the remaining material was
704 pelleted using a tabletop centrifuge for 2 min at 16,000 × *g*. Subsequently, a
705 portion of the supernatant fluid was removed and combined 1:1 with a 5 μM

solution of SYTOX Green nucleic acid stain (Thermo Fisher), followed by measurement of fluorescence (excitation/emission: 504/523 nm) using a fluorescence-capable Synergy 2 plate reader from BioTek (Winooski, VT). A standard curve was established using a known DNA solution and the results were calculated as ng of eDNA released per CFU of the biofilm.

Quantitative reverse transcription PCR (qRT-PCR). Total RNA was extracted from *S. mutans* cells harvested at $OD_{600} \approx 0.5$ using an RNeasy kit (Qiagen) by following an established protocol (49). Primers specific to *sppA* were used for both the reverse transcription and Real-time PCR that followed, with *gyrA* serving as an internal control (25).

Acknowledgment

This work was supported by DE12236 from the National Institute of Dental and Craniofacial Research.

References

1. Postma PW, Lengeler JW, Jacobson GR. 1993. Phosphoenolpyruvate:carbohydrate phosphotransferase systems of bacteria. Microbiol Rev 57:543-94.
2. Irani MH, Maitra PK. 1977. Properties of *Escherichia coli* mutants deficient in enzymes of glycolysis. J Bacteriol 132:398-410.

3. Zeng L, Chakraborty B, Farivar T, Burne RA. 2017. Coordinated regulation of the EII^{Man} and *fruRKI* operons of *Streptococcus mutans* by global and fructose-specific pathways. Appl Environ Microbiol 83.

4. Zeng L, Farivar T, Burne RA. 2016. Amino sugars enhance competitiveness of beneficial commensals with *Streptococcus mutans* through multiple mechanisms. Appl Environ Microbiol 82:3671-82.

5. Maleki S, Hrudikova R, Zotchev SB, Ertesvåg H. 2017. Identification of a new phosphatase enzyme potentially involved in the sugar phosphate stress response in *Pseudomonas fluorescens*. Applied and Environmental Microbiology 83.

6. Richards GR, Patel MV, Lloyd CR, Vanderpool CK. 2013. Depletion of glycolytic intermediates plays a key role in glucose-phosphate stress in *Escherichia coli*. J Bacteriol 195:4816-25.

7. Korithoski B, Levesque CM, Cvitkovitch DG. 2007. Involvement of the detoxifying enzyme lactoylglutathione lyase in *Streptococcus mutans* aciduricity. J Bacteriol 189:7586-92.

8. Kadner RJ, Murphy GP, Stephens CM. 1992. Two mechanisms for growth inhibition by elevated transport of sugar phosphates in *Escherichia coli*. J Gen Microbiol 138:2007-14.

9. Assev S, Rolla G. 1986. Further studies on the growth inhibition of *Streptococcus mutans* OMZ 176 by xylitol. Acta Pathol Microbiol Immunol Scand B 94:97-102.

10. Vanderpool CK. 2007. Physiological consequences of small RNA-mediated regulation of glucose-phosphate stress. Curr Opin Microbiol 10:146-51.

11. Tanzer JM, Thompson A, Wen ZT, Burne RA. 2006. *Streptococcus mutans*: fructose transport, xylitol resistance, and virulence. J Dent Res 85:369-73.

12. Trahan L. 1995. Xylitol: a review of its action on mutans streptococci and dental plaque--its clinical significance. Int Dent J 45:77-92.

13. Trahan L, Neron S, Bareil M. 1991. Intracellular xylitol-phosphate hydrolysis and efflux of xylitol in *Streptococcus sobrinus*. Oral Microbiol Immunol 6:41-50.

14. Miyasawa-Hori H, Aizawa S, Takahashi N. 2006. Difference in the xylitol sensitivity of acid production among *Streptococcus mutans* strains and the biochemical mechanism. Oral Microbiol Immunol 21:201-5.

15. Soderling E, Alaraisanen L, Scheinin A, Makinen KK. 1987. Effect of xylitol and sorbitol on polysaccharide production by and adhesive properties of *Streptococcus mutans*. Caries Res 21:109-16.

16. Soderling EM, Hietala-Lenkkeri AM. 2010. Xylitol and erythritol decrease adherence of polysaccharide-producing oral streptococci. Curr Microbiol 60:25-9.

17. Trahan L, Mouton C. 1987. Selection for *Streptococcus mutans* with an altered xylitol transport capacity in chronic xylitol consumers. J Dent Res 66:982-8.

18. Wen ZT, Browngardt C, Burne RA. 2001. Characterization of two operons that encode components of fructose-specific enzyme II of the sugar:phosphotransferase system of *Streptococcus mutans*. FEMS Microbiol Lett 205:337-42.

19. Dills SS, Seno S. 1983. Regulation of hexitol catabolism in *Streptococcus mutans*. J Bacteriol 153:861-6.

20. Cvitkovitch DG, Boyd DA, Hamilton IR. 1995. Regulation of sugar transport via the multiple sugar metabolism operon of *Streptococcus mutans* by the phosphoenolpyruvate phosphotransferase system. J Bacteriol 177:5704-6.

21. Coleman JE. 1992. Structure and mechanism of alkaline phosphatase. Annu Rev Biophys Biomol Struct 21:441-83.

22. Dashper SG, Reynolds EC. 1992. pH regulation by *Streptococcus mutans*. J Dent Res 71:1159-65.

23. Thompson J, Chassy BM. 1983. Intracellular hexose-6-phosphate:phosphohydrolase from *Streptococcus lactis*: purification, properties, and function. J Bacteriol 156:70-80.

24. Kuznetsova E, Proudfoot M, Gonzalez CF, Brown G, Omelchenko MV, Borozan I, Carmel L, Wolf YI, Mori H, Savchenko AV, Arrowsmith CH, Koonin EV, Edwards AM, Yakunin AF. 2006. Genome-wide analysis of substrate specificities of the *Escherichia coli* haloacid dehalogenase-like phosphatase family. J Biol Chem 281:36149-61.

25. Zeng L, Burne RA. 2015. Sucrose- and fructose-specific effects on the transcriptome of *Streptococcus mutans*, as determined by RNA sequencing. Appl Environ Microbiol 82:146-56.

26. Abranches J, Chen YY, Burne RA. 2003. Characterization of *Streptococcus mutans* strains deficient in EIIAB^{Man} of the sugar phosphotransferase system. Appl Environ Microbiol 69:4760-9.

27. Abranches J, Nascimento MM, Zeng L, Browngardt CM, Wen ZT, Rivera MF, Burne RA. 2008. CcpA regulates central metabolism and virulence gene expression in *Streptococcus mutans*. J Bacteriol 190:2340-9.

28. Huynh K, Partch CL. 2015. Analysis of protein stability and ligand interactions by thermal shift assay. Curr Protoc Protein Sci 79:28.9.1-14.

29. Liao S, Klein MI, Heim KP, Fan Y, Bitoun JP, Ahn SJ, Burne RA, Koo H, Brady LJ, Wen ZT. 2014. *Streptococcus mutans* extracellular DNA is upregulated during growth in biofilms, actively released via membrane vesicles, and influenced by components of the protein secretion machinery. J Bacteriol 196:2355-66.

30. Cornejo OE, Lefebure T, Pavinski Bitar PD, Lang P, Richards VP, Eilertson K, Do T, Beighton D, Zeng L, Ahn SJ, Burne RA, Siepel A, Bustamante CD, Stanhope MJ. 2013. Evolutionary and population genomics of the cavity causing bacteria *Streptococcus mutans*. Mol Biol Evol 30:881-93.

31. Pihlanto-Leppala A, Soderling E, Makinen KK. 1990. Expulsion mechanism of xylitol 5-phosphate in *Streptococcus mutans*. Scand J Dent Res 98:112-9.

32. Zeng L, Das S, Burne RA. 2010. Utilization of lactose and galactose by *Streptococcus mutans*: transport, toxicity, and carbon catabolite repression. J Bacteriol 192:2434-44.

33. Calderone V, Forleo C, Benvenuti M, Thaller MC, Rossolini GM, Mangani S. 2006. A structure-based proposal for the catalytic mechanism of the bacterial acid phosphatase AphA belonging to the DDDD superfamily of phosphohydrolases. Journal of Molecular Biology 355:708-721.

34. Thaller MC, Schippa S, Rossolini GM. 1998. Conserved sequence motifs among bacterial, eukaryotic, and archaeal phosphatases that define a new phosphohydrolase superfamily. Protein Sci 7:1647-52.

35. Horler RS, Vanderpool CK. 2009. Homologs of the small RNA SgrS are broadly distributed in enteric bacteria but have diverged in size and sequence. Nucleic Acids Res 37:5465-76.

36. Kessler JR, Cobe BL, Richards GR. 2017. Stringent response regulators contribute to recovery from glucose phosphate stress in *Escherichia coli*. Applied and Environmental Microbiology 83.

37. Klein MI, Hwang G, Santos PH, Campanella OH, Koo H. 2015. *Streptococcus mutans*-derived extracellular matrix in cariogenic oral biofilms. Front Cell Infect Microbiol 5:10.

38. Tanzer JM, Chassy BM, Krichevsky MI. 1971. Sucrose metabolism by *Streptococcus mutans*, SL-I. Biochim Biophys Acta 261:379-87.

39. Zeng L, Burne RA. 2013. Comprehensive mutational analysis of sucrose-metabolizing pathways in *Streptococcus mutans* reveals novel roles for the sucrose phosphotransferase system permease. J Bacteriol 195:833-43.

40. Ahn SJ, Rice KC, Oleas J, Bayles KW, Burne RA. 2010. The *Streptococcus mutans* Cid and Lrg systems modulate virulence traits in response to multiple environmental signals. Microbiology 156:3136-47.

41. Seaton K, Ahn SJ, Sagstetter AM, Burne RA. 2011. A transcriptional regulator and ABC transporters link stress tolerance, (p)ppGpp, and genetic competence in *Streptococcus mutans*. J Bacteriol 193:862-74.

42. Burne RA, Wen ZT, Chen YY, Penders JE. 1999. Regulation of expression of the fructan hydrolase gene of *Streptococcus mutans* GS-5 by induction and carbon catabolite repression. J Bacteriol 181:2863-71.

43. Wen ZT, Yates D, Ahn SJ, Burne RA. 2010. Biofilm formation and virulence expression by *Streptococcus mutans* are altered when grown in dual-species model. BMC Microbiol 10:111.

44. Sambrook J, Russell DW. 2001. Molecular cloning: a laboratory manual, 3rd ed. Cold Spring Harbor Laboratory Press, Cold Spring Harbor, N.Y.

45. Biswas I, Jha JK, Fromm N. 2008. Shuttle expression plasmids for genetic studies in *Streptococcus mutans*. Microbiology 154:2275-82.

46. Zeng L, Burne RA. 2008. Multiple sugar: phosphotransferase system permeases participate in catabolite modification of gene expression in *Streptococcus mutans*. Mol Microbiol 70:197-208.

47. Zeng L, Burne RA. 2015. NagR differentially regulates the expression of the *glmS* and *nagAB* genes required for amino sugar metabolism by *Streptococcus mutans*. J Bacteriol 197:3533-44.

48. Loo CY, Corliss DA, Ganeshkumar N. 2000. *Streptococcus gordonii* biofilm formation: identification of genes that code for biofilm phenotypes. J Bacteriol 182:1374-82.

49. Ahn SJ, Lemos JA, Burne RA. 2005. Role of HtrA in growth and competence of *Streptococcus mutans* UA159. J Bacteriol 187:3028-38.

50. Ajdic D, McShan WM, McLaughlin RE, Savic G, Chang J, Carson MB, Primeaux C, Tian R, Kenton S, Jia H, Lin S, Qian Y, Li S, Zhu H, Najar F, Lai H, White J, Roe BA, Ferretti JJ. 2002. Genome sequence of *Streptococcus mutans* UA159, a cariogenic dental pathogen. Proc Natl Acad Sci U S A 99:14434-9.

878 **Figure legends**

879 **FIGURE 1** Overexpression of *sppA* enhances growth of a *fruK* mutant on
880 fructose. (A) Relative *sppA* mRNA levels measured in UA159/pIB184,
881 UA159/pIB508, FruK-13/pIB184, and FruK-13/pIB508. Cultures were prepared
882 using BHI medium and harvested at the exponential phase. Quantitative reverse
883 transcription PCR (qRT-PCR) was carried out using the total RNA samples, and
884 the relative abundance of *sppA* was determined using the ΔΔCq method. The
885 error bars denote the standard deviations. Student's *t*-test was performed to
886 determine the statistical significance of the data, with asterisks denoting $P < 0.05$.
887 (B) FruK-13/pIB508 (red squares) and FruK-13/pIB184 (blue diamonds) were
888 cultivated in BHI and then diluted into TV medium containing 10 mM fructose.
889 The cultures were overlaid with mineral oil and OD_{600} was measured every 30
890 min in a Bioscreen C. The results represent the average of at least three
891 biological replicates.

892

893 **FIGURE 2** *In vitro* characterization of SppA as a hexose-phosphate:
894 phosphohydrolase. The majority of the reactions (except panels B&C) were
895 performed at 37°C in a basic buffer composed of 50 mM PIPES (pH 6.5), 5 mM
896 $MgCl_2$, and 1 mM $MnCl_2$. Release of phosphate was measured using a Malachite
897 Green Reagent (MGR), and the results were divided by time and amounts of
898 enzyme (A, D), or normalized for relative activities (B, C). (A) 10 mM of the
899 indicated sugar-phosphates were incubated with His-SppA (0.08 μM for F-1-P,
900 0.67 μM for the rest), with release of phosphate being monitored over a period of

10 min. (B) 0.1 mM of F-1-P was incubated for 5 min with 0.33 µM of His-SppA and the specified amounts of metal ions. (C) 0.67 mM F-1-P was incubated with 0.04 µM of His-SppA for 130 sec at the indicated pH values (See Methods for details). (D) Increasing concentrations of F-1-P and F-6-P were each mixed with His-SppA and phosphate release was monitored over defined periods of time (See Methods for details).

FIGURE 3 Transcription of the *spp* operon is regulated by SppR, fructose derivatives and the PTS. The P*sppR::cat* fusion was integrated into the chromosome of the wild type (A) or various mutants (B) to monitor the expression of the operon. All strains were first cultivated to mid-exponential phase (OD_{600} = 0.3 to 0.4) in a TV medium with 10 mM glucose, then (A) 25 or 50 mM of the specified carbohydrates, or (B) 50 mM of glucose or fructose was added, the cultures were incubated for 1 h, and cells were harvested for CAT assays. Error bars denote standard deviations. Asterisks indicate statistically significant difference (by Student's *t*-test, P <0.05) in comparison (A) with glucose at the same concentrations, or (B) with the wild type (WT) treated with the same carbohydrates.

FIGURE 4 *In vitro* interactions of SppR with the *spp* promoter region or F-6-P. (A) EMSA using recombinant His-SppR and a biotin-labeled probe containing the promoter region of *sppR.* His-SppR (0.05 to 1 µM) was incubated with 0.4 nM of DNA probe in a 10-µl reaction for 30 min, before the mixture was resolved on a

non-denaturing polyacrylamide gel. Certain reactions also contained 0.4 μM of unlabeled probe as a competitor, or 5 mM of the specified sugar phosphate. (B) The melting temperatures (Tm) of His-SppR in the presence of varying amounts of F-6-P. A small amount of SYPRO Orange was added to monitor the thermal denaturation of the protein.

FIGURE 5 Overexpression of SppA enhances resistance to xylitol. Growth phenotypes of various strains were monitored over time in a Bioscreen C (A, B), or by measuring the final yield (OD_{600}) after overnight incubation (C). Strains were cultivated first on BHI to exponential phase, then diluted using TV medium containing 0.5% glucose in addition to (A, B) 1% xylitol, or (C) the amounts of xylitol specified on the *x*-axis.

FIGURE 6 Fructose metabolism alters biofilm development by *S. mutans.* BM containing 2 mM sucrose and 18 mM glucose (BMGS) or 18 mM fructose (BMFS) was used for biofilm development. (A) Wild type UA159 and its isogenic mutants *levD* and *fruI* were each incubated for 24 h and the amounts of biofilms formed were visualized and quantified by crystal violet staining. (B) Biofilms formed by UA159 were treated with a LIVE/DEAD vitality stain and visualized under a confocal laser-scanning microscope, with green indicating live cells and red indicating dead cells. (C) eDNA released from 48-h biofilms formed by strains UA159/pIB184 (blue) and UA159/pIB508 (orange) were quantified using a DNA dye (SytoX Green) and a standard curve. The results were normalized using total CFU from each sample (D). Error bars represent standard deviations. Statistical

948 analysis was performed using Student's *t* test, with asterisks denoting *P* values: *
949 <0.05, ** <0.005, and *** <0.0005.
950
951 **FIGURE 7** HAD family phosphatases contribute to sugar-phosphate tolerance.
952 (A) *S. mutans* UA159 and its mutants deficient in putative phosphohydrolases.
953 (B) UA159, a *lacD* mutant, and *lacD* derivatives containing plasmid pIB428 that
954 overexpresses SMU.428 or the vector pIB184. Bacterial cultures were each
955 prepared in BHI, then diluted into TV base medium supplemented with (A) 0.5%
956 glucose and various amounts of xylitol or (B) 0.5% sorbitol and various amounts
957 of galactose. After 17 to 20 h incubation at 37°C, OD_{600} of the cultures were
958 recorded. Results are the averages of at least three independent cultures, with
959 error bars denoting the standard deviations.

960 **Table 1.** Bacterial strains and plasmids used in this study.

Strains	Relevant genotypes[a]	Source or reference
Streptococcus mutans		
UA159	Wild type, serotype *c*	(50)
FruK-13	*fruK*M28stop	(3)
MMZ1387	UA159 *sppR*::Km^r	This study
MMZ1388	UA159 *sppR*::Em^r	This study
MMZ1399	UA159 *sppA*::Km^r	This study
MMZ1400	UA159 *sppA*::Em^r	This study
MMZ1416	UA159 P*sppR::cat*	This study
MMZ1518	*levD*::Em^r P*sppR::cat*	This study
MMZ1519	*fruI*::Sp^r P*sppR::cat*	This study
MMZ1520	*manL*::Em^r P*sppR::cat*	This study
MMZ1521	*ccpA*::Sp^r P*sppR::cat*	This study
MMZ1549	UA159 SMU.428::Km^r	This study
MMZ1551	UA159 SMU.718c::Km^r	This study
MMZ1570	UA159 SMU.488::Km^r	This study
MMZ1573	*sppR*::Em^r P*sppR::cat*	This study
MMZ1574	*sppA*::Em^r P*sppR::cat*	This study
Plasmids		
pIB184	Shuttle expression vector	(45)
pIB508	*sppA* cloned into pIB184	This study
pIB428	SMU.428 cloned into pIB184	This study

961 [a] Km^r kanamycin resistance; Sp^r, spectinomycin resistance; Em^r, erythromycin

962 resistance.

963 **Table 2.** Primers used in this study.

Primers	Sequence[a]	Purpose
SMU.507-1	5'- GGT TGG GAT AGT GAT AAA TCG CAT -3'	Deleting *sppR*
SMU.507-2GA	5'- GCC ATT TAT TAT TTC CTT CCT CTT TTA GTT CTT GAT ACA TAA CTT TCC TCT TTT C -3'	Deleting *sppR*
SMU.507-3GA	5'- ATA TTT TAC TGG ATG AAT TGT TTT AGT AGA CGG GCA AAT TTA TCT GAT AAG GT -3'	Deleting *sppR*
SMU.507-4	5'- GCC TGT GCA TTG GCA ATT AAG A -3'	Deleting *sppR*
SMU.508-S	5'- ATG GGG CTC TGA TTG TTG AG -3'	qRT-PCR
SMU.508-AS	5'- GCG GAA ACT GCT TCT TGA TT -3'	qRT-PCR
SMU.508-5'Bm	5'- CGA GTA AAA GGA TCC GGG CAA ATT TAT CT -3'	pIB508
SMU.508-3'SacI	5'- AAC CAC TTG AGC TCT GTT TTA AAT TAA AAC A -3'	pIB508
SMU.508-1	5'- CGT CGT GAT TTT GCT CTT TTG A -3'	Deleting *sppA*
SMU.508-2GA	5'- GCC ATT TAT TAT TTC CTT CCT CTT TTA CTT TGC CAT AAC AAA CCC C-3'	Deleting *sppA*
SMU.508-3GA	5'- ATA TTT TAC TGG ATG AAT TGT TTT AGT AGG ACA ACG GTG TTT CCA AGG TG-3'	Deleting *sppA*
SMU.508-4	5'- CGA GAC ATA TCA GCA GGA TTG AT -3'	Deleting *sppA*
P507-3'Bm	5'- GTT CTT GAT ACA TAG GAT CCC TCT TTT CA -3'	P*sppR::cat* fusion
P507-5'SacI	5'- AAC TTG TAG GAG CTC TCA TAA GTC ATC AA -3'	P*sppR::cat* fusion
SMU.507-5'Bm	5'- TGA AAA GAG GGG ATC CAT GTA TCA AGA ACA -3'	His-SppR

SMU.507-5'HIII	5'- CAC TTA AAA TAA GCT TAA TTG TCT TTG CCA -3'	His-SppR
SMU.508-5'Bm	5'- AAA GGG ATC CGT TAT GGC AAA GAC AAT TAA -3'	His-SppA
SMU.508-3'HIII	5'- CAA AAA ATC AAG CTT CAA AAA CCA CTT GA -3'	His-SppA
SMU.507-EMSA-5'	5'- GCG TGC CAG CGA CCT CCT ATT CCT CTT TTG CTA ATG TTA TCT -3'	DNA probe
SMU.507-EMSA-3'	5'- GTT CTT GAT ACA TAA CTT TCC TCT TTT CA -3'	DNA probe
SMU.428-1	5'- CCA TGG GCT CTG GAA CA -3'	Deleting SMU.428
SMU.428-2GA	5'- GCC ATT TAT TAT TTC CTT CCT CTT TTA GCG TGC CAT CCA TAT CAA TAG CA -3'	Deleting SMU.428
SMU.428-3GA	5'- ATA TTT TAC TGG ATG AAT TGT TTT AGT AGA GCT GGT GTT GCT CAA GCT -3'	Deleting SMU.428
SMU.428-4	5'- GGC CAT ACT AAC GTA CAG CA -3'	Deleting SMU.428
SMU.718c-1	5'- GGG TTA CCC TAG AAG ACT ATC TTA GT -3'	Deleting SMU.718c
SMU.718c-2GA	5'- GCC ATT TAT TAT TTC CTT CCT CTT TTA GCC GTC AAT ATC GAC AGC AAC C -3'	Deleting SMU.718c
SMU.718c-3GA	5'- ATA TTT TAC TGG ATG AAT TGT TTT AGT AGA CAG TGG GGT CGC TTA TGC A -3'	Deleting SMU.718c
SMU.718c-4	5'- GAC TAG CCA AAG TAA TGA AAG AGT GT -3'	Deleting SMU.718c
SMU.488-1	5'- GGG TTG TTA TGG ATA TCC ATG TAC -3'	Deleting SMU.488
SMU.488-2GA	5'- GCC ATT TAT TAT TTC CTT CCT CTT TTA CCC GTA TCT TTG ATG CGT AAG -3'	Deleting SMU.488
SMU.488-3GA	5'- ATA TTT TAC TGG ATG AAT TGT TTT AGT AGA GAG AGC ATC GAG GTG ATT GAT -3'	Deleting SMU.488
SMU.488-4	5'- CCA AAA CAT TCA TTA TGC CTT TAC GCA -3'	Deleting SMU.488

SMU.428-5'Bm	5'- GCT GTG CCA GGA TCC TCG ATT TGT GAT ACA CTA -3'	pIB428
SMU.428-3'RI	5'- GAT AAA AAC GAA TTC CCA GTT CCT TTT TCA TGA -3'	pIB428

[a] An insertion or mutation is indicated by underlining.

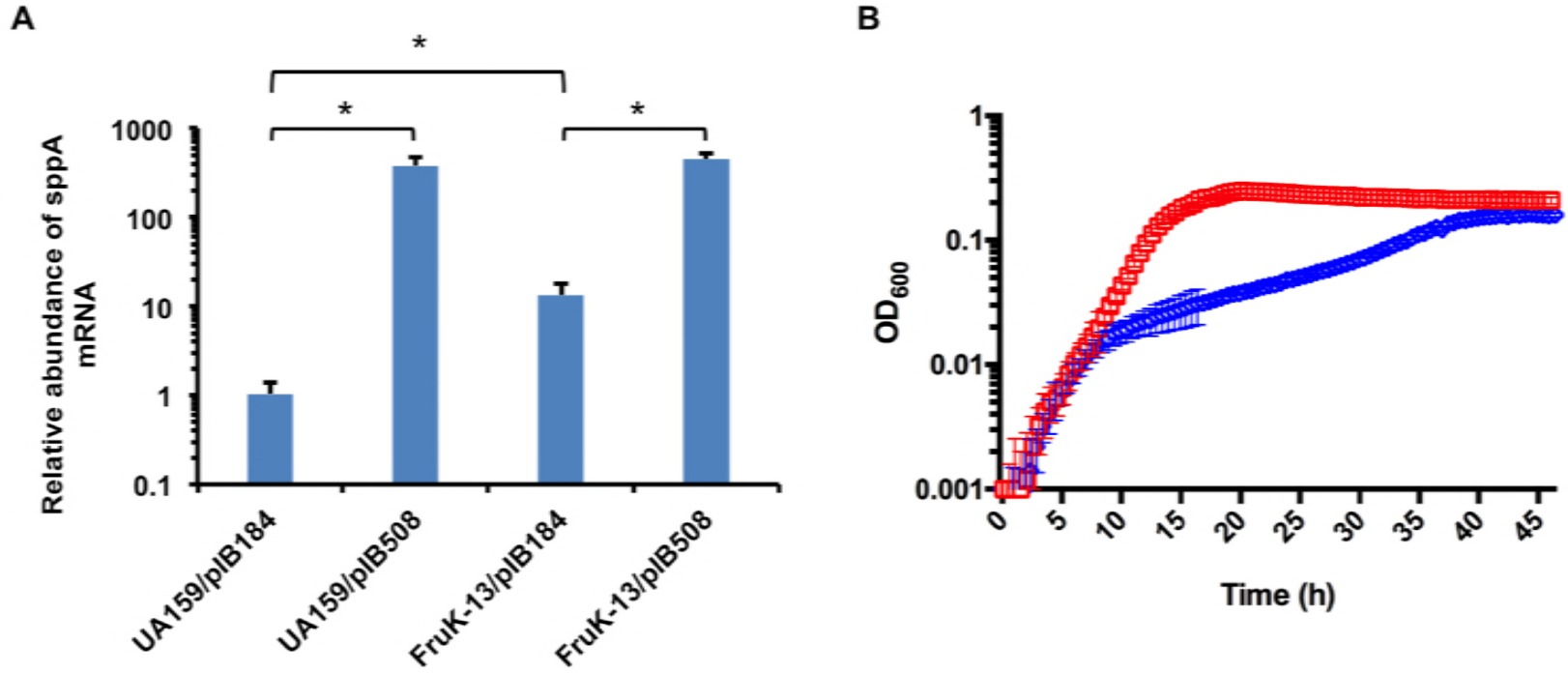
A
*
*
*
1000
100
10
1
0.1
Relative abundance of sppA mRNA
UA159/pIB184
UA159/pIB508
FruK-13/pIB184
FruK-13/pIB508
B
1
0.1
0.01
0.001
OD600
0
5
10
15
20
25
30
35
40
45
Time (h)

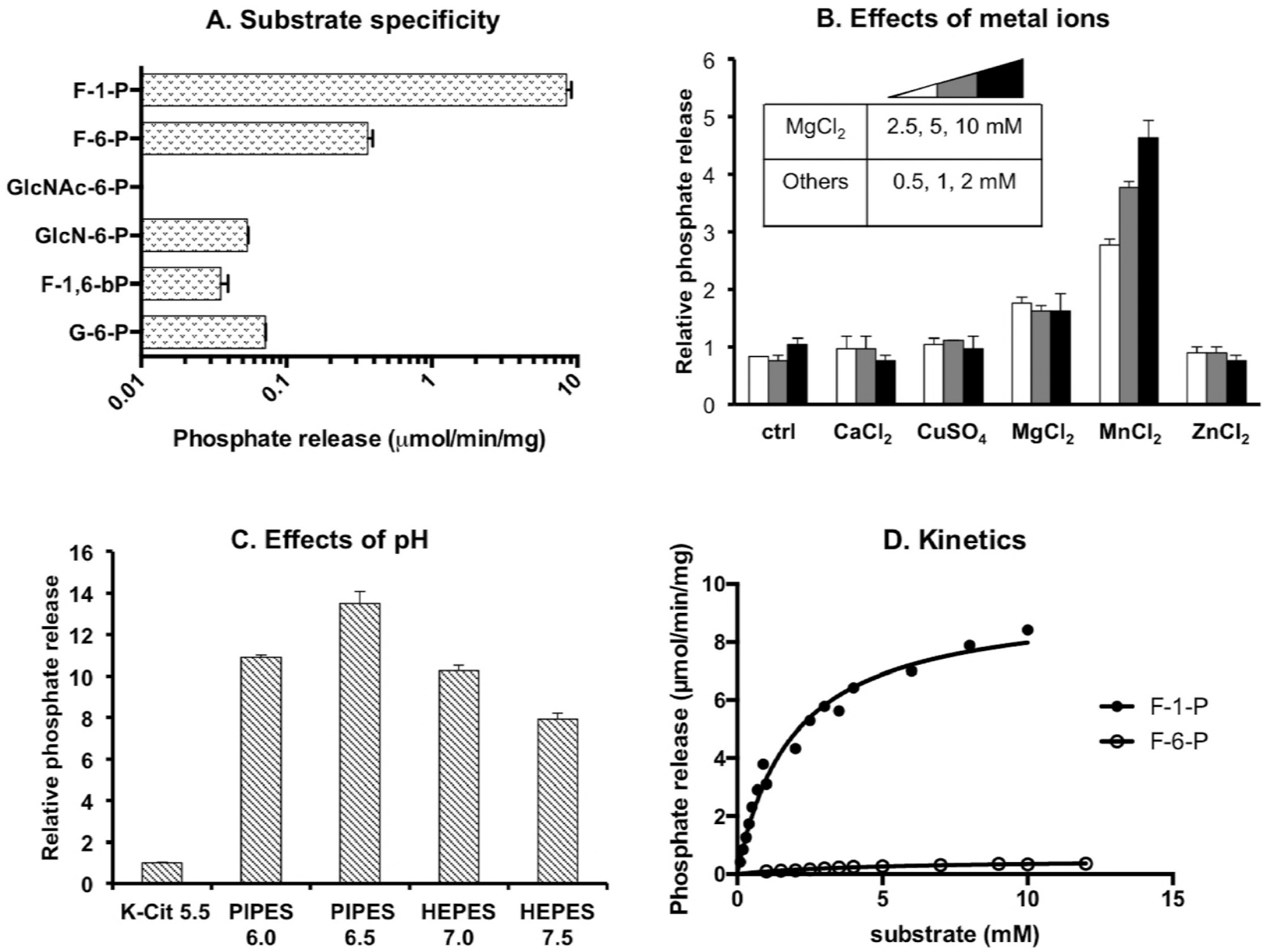
A. Substrate specificity
F-1-P
F-6-P
GlcNAc-6-P
GlcN-6-P
F-1,6-bP
G-6-P
0.01
0.1
1
10
Phosphate release (μmol/min/mg)
B. Effects of metal ions
MgCl2
2.5, 5, 10 mM
Others
0.5, 1, 2 mM
Relative phosphate release
ctrl
CaCl2
CuSO4
MgCl2
MnCl2
ZnCl2
C. Effects of pH
Relative phosphate release
K-Cit 5.5
PIPES 6.0
PIPES 6.5
HEPES 7.0
HEPES 7.5
D. Kinetics
Phosphate release (μmol/min/mg)
substrate (mM)
F-1-P
F-6-P

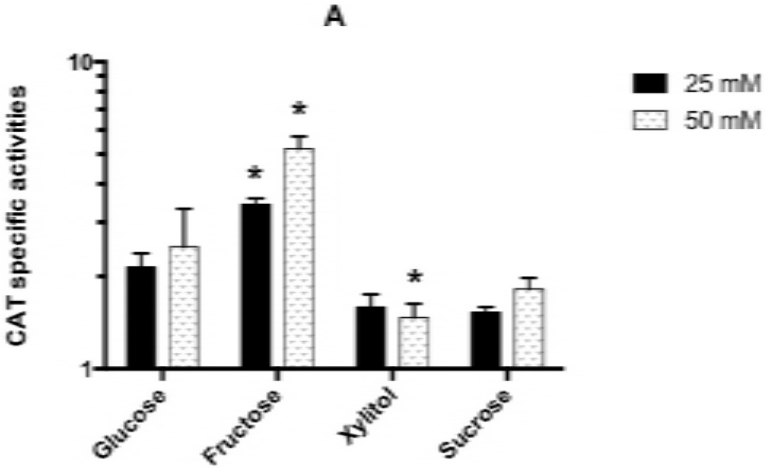
A
CAT specific activities
10
1
25 mM
50 mM
Glucose
Fructose
Xylitol
Sucrose

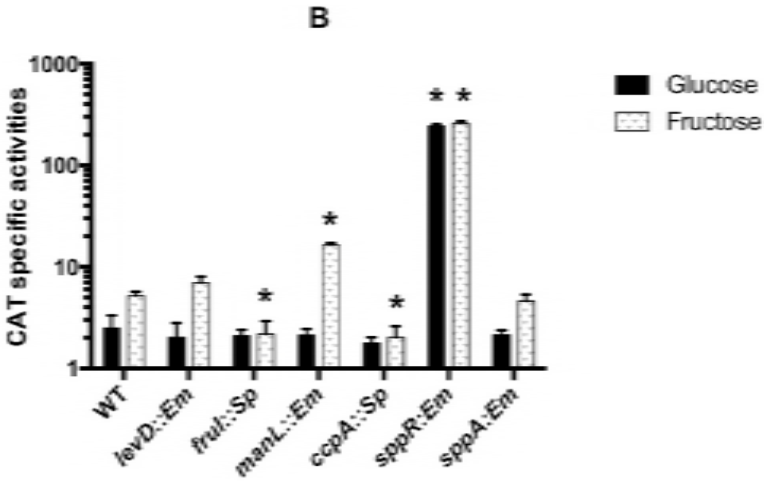
B
CAT specific activities
1000
100
10
1
Glucose
Fructose
WT
levD::Em
fruI::Sp
manL::Em
ccpA::Sp
sppR:Em
sppA:Em

A

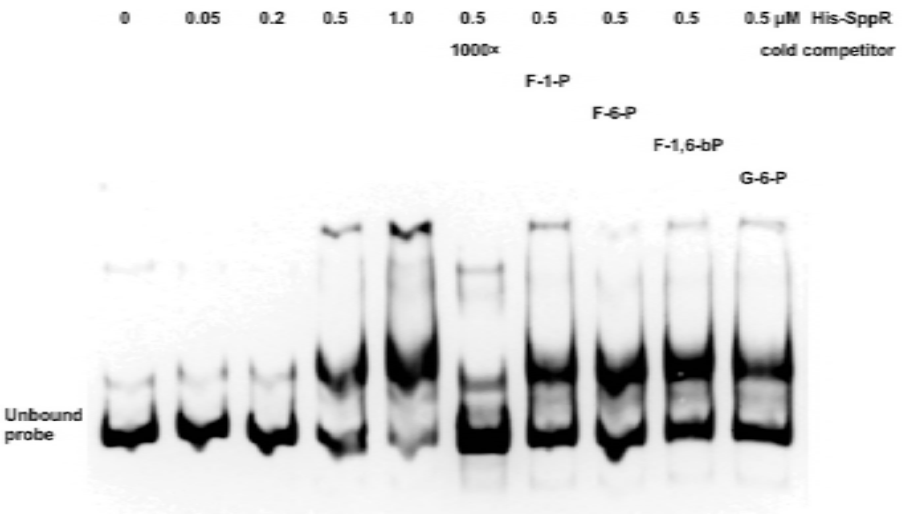
0
0.05
0.2
0.5
1.0
0.5
0.5
0.5
0.5
0.5 μM His-SppR
1000×
cold competitor
F-1-P
F-6-P
F-1,6-bP
G-6-P
Unbound probe

B

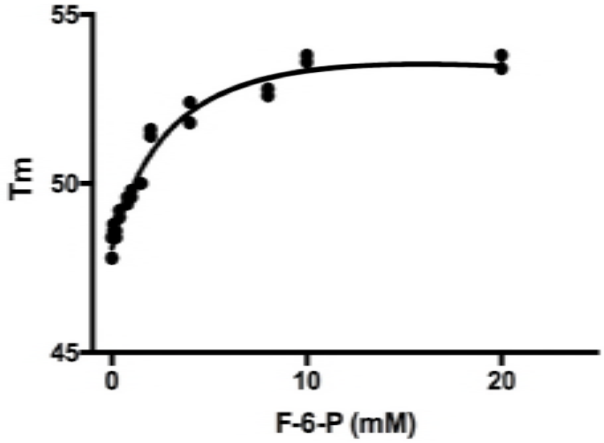
55
50
45
Tm
0
10
20
F-6-P (mM)

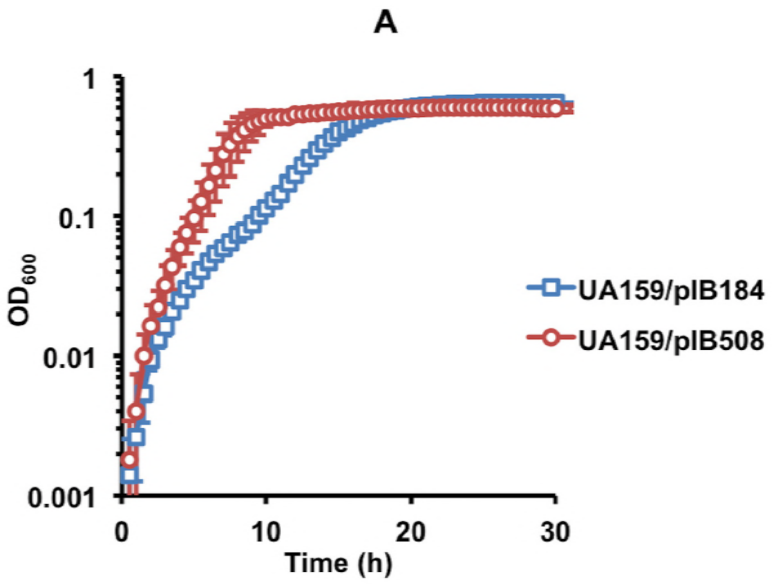
A
1
0.1
0.01
0.001
OD600
0
10
20
30
Time (h)
UA159/pIB184
UA159/pIB508

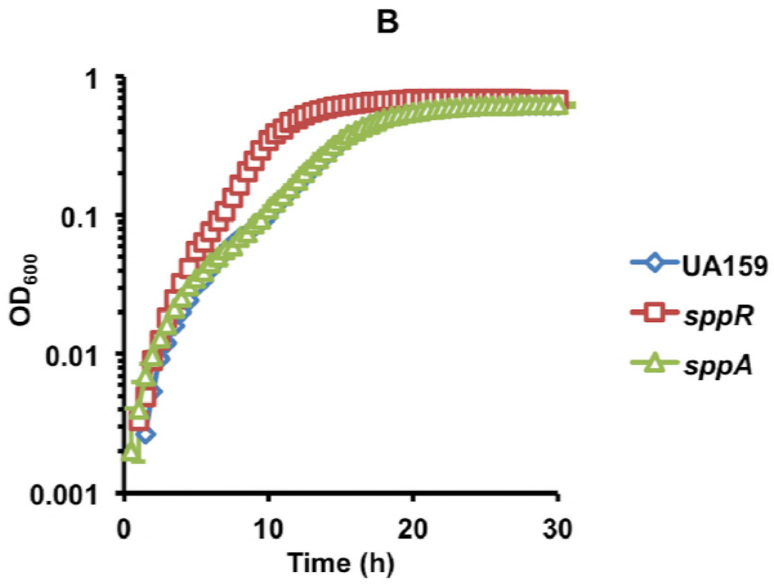
B
1
0.1
0.01
0.001
OD600
0
10
20
30
Time (h)
UA159
sppR
sppA

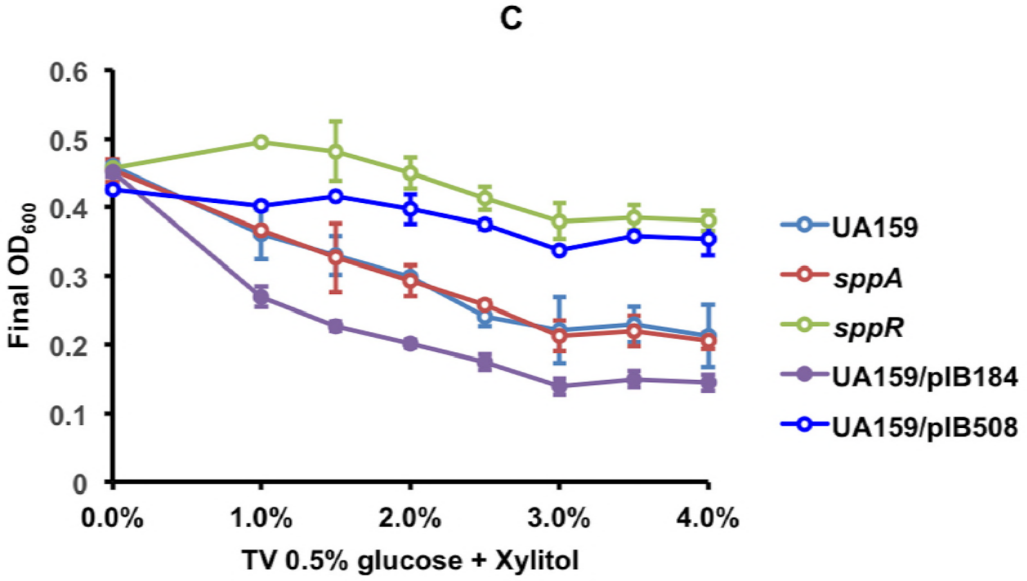
C
0.6
0.5
0.4
0.3
0.2
0.1
0
Final OD600
0.0%
1.0%
2.0%
3.0%
4.0%
TV 0.5% glucose + Xylitol
UA159
sppA
sppR
UA159/pIB184
UA159/pIB508

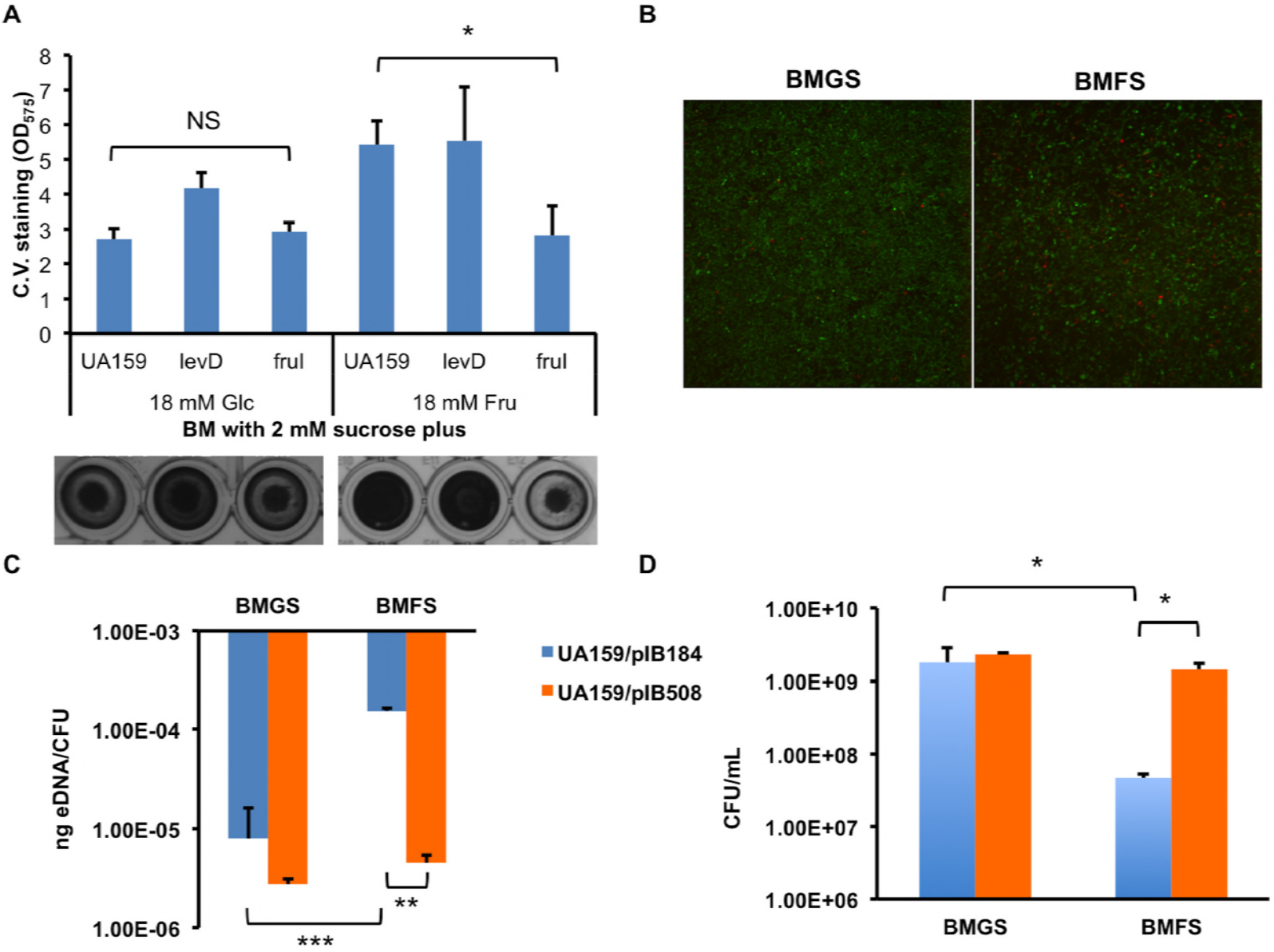
A
B
C
D
C.V. staining (OD_{575})
NS
*
UA159
levD
fruI
18 mM Glc
18 mM Fru
BM with 2 mM sucrose plus
BMGS
BMFS
ng eDNA/CFU
1.00E-03
1.00E-04
1.00E-05
1.00E-06
***
**
UA159/pIB184
UA159/pIB508
CFU/mL
1.00E+10
1.00E+09
1.00E+08
1.00E+07
1.00E+06

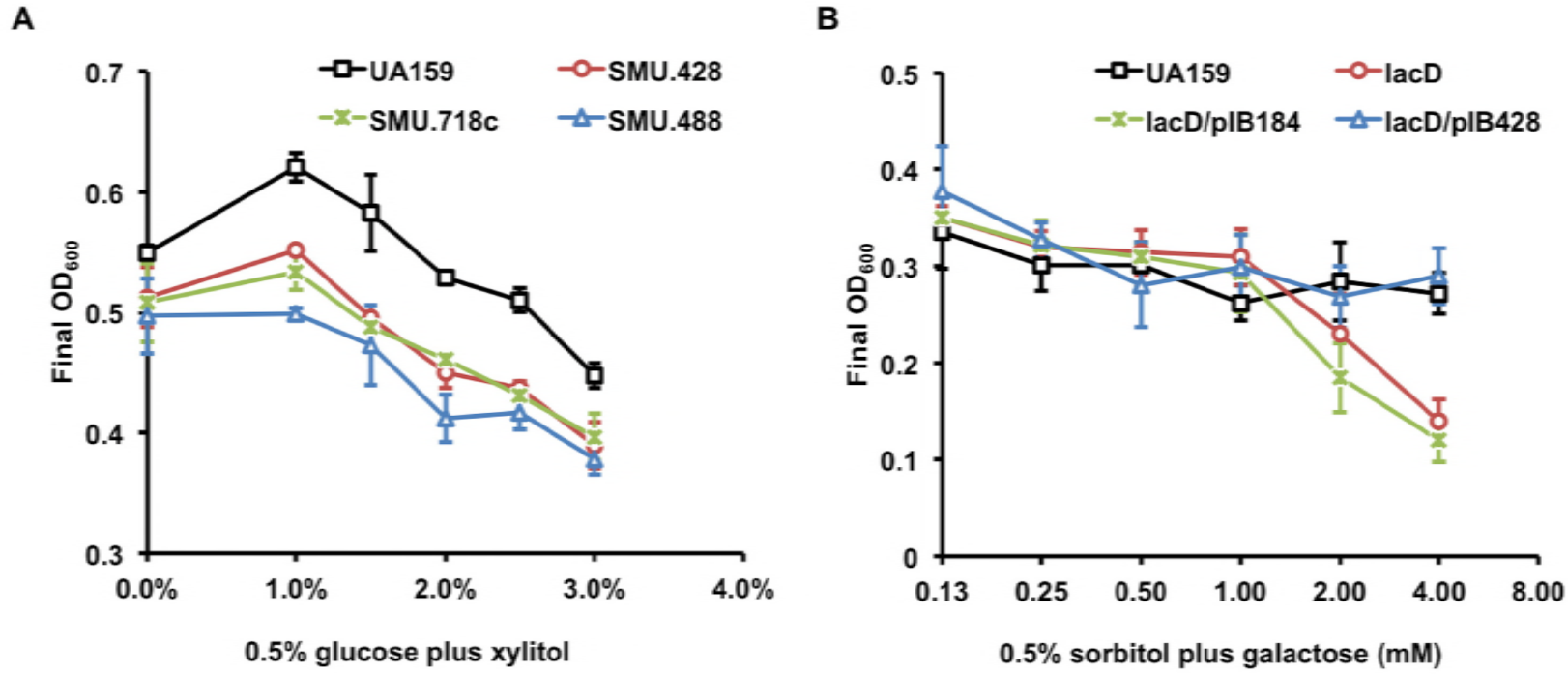
A
UA159
SMU.428
SMU.718c
SMU.488
Final OD600
0.7
0.6
0.5
0.4
0.3
0.0%
1.0%
2.0%
3.0%
4.0%
0.5% glucose plus xylitol
B
UA159
lacD
lacD/pIB184
lacD/pIB428
Final OD600
0.5
0.4
0.3
0.2
0.1
0
0.13
0.25
0.50
1.00
2.00
4.00
8.00
0.5% sorbitol plus galactose (mM)